



Finding your car in the car park; Only use a smartphone

Zhao Liu ^{1,*}, Weiwei Chen ², Zhigang Li ³

^{1, 2, 3} Command and Information System Department, PLA University of Science and Technology, Nanjing, China

Index Terms

Indoor Positioning
Smart-phone Sensor
Pedestrian Dead Reckoning
Magnetic Information

Abstract— As we know, remembering where a car is parked in a large parking port is very difficult. Even with an indoor positioning system, if we don't mark the car's position previously, it can be hard to get back to the car. This paper presents a solution based on magnetic information matching and Pedestrian Dead Reckoning (PDR) to improve the situation. By recording the user's moving trace with pedestrian dead reckoning and using magnetic information matching to find the right turning direction at the turning point, this paper brings up a new way to find the user's car in a car park without using pre-deployed infrastructure or radio signals. The experiments show that the new solution can navigate the user back to the car successfully.

Received: 5 May 2016

Accepted: 29 May 2016

Published: 21 June 2016

© 2016 The Author(s). Published by TAF Publishing.

I. INTRODUCTION

As we know, it's often a difficult problem to get back to our car in a large, underground parking lot. Researchers have developed indoor positioning systems [1], [2]. But most can't work well in this scene. Firstly, many solutions need large scale of pre-deployed instructions or pre-works. For example, the RFID way needs to deploy the RFID tags in advance [3], which is expensive and inefficient; the WiFi method [4] is unusable in place where WiFi signal is rare; and the PDR technology usually needs an indoor map [5] which is difficult to get most of the time. Secondly, if we have a map of the car park, we have to mark the car's position on the map so that we can get back with the help of the map, but there are many similar cars and similar parking places in a car park, it's not easy to mark you car position on the map.

To allocate these two problems we review the situation in a car park. If a user wants to return to the car, there must be a process in which the user walks to the present place from the car position. If we record the walk path, we can go back to the car's position along the record path. By surveying the present work in this filed, we find that the Pedestrian Dead Reckoning (PDR) technology can record the user's move path and infer the user's position [6], [7], So we consider using PDR technology to solve the problem.

But there are still two problems when using PDR technology, one is the cumulative error and other is the turning point. In the previous works researchers used WiFi/RFID signal or map to allocate these two problems, but as said at the beginning the RFID tags are expensive and WiFi fingerprint or indoor map is hard to get, we have to make use of some other information. As the magnetic field is stalely widespread everywhere [8], we can use it to replace the above things.

This paper mainly promotes a method to choose the

*Corresponding author: Zhao Liu
E-mail: lz_mail_pust@163.com



right turning direction at the turning point. We calculated the similarity of several magnetic information groups with a new magnetic information matching algorithm and got the most similar one with stand for the right direction. We used the turning point to depart the user's path into several sections to decrease the error's accumulation and get the turning direction using magnetic information matching. Thus navigate the user back to the car. Through several experiments, our solution can navigate back successfully.

II. RELATED WORK

The current researches have put forward many navigation and location systems based on smartphones which are mainly in two ways: WiFi signal and PDR. The Pazl [4] collects the indoor WiFi information, locates the user by matching the WiFi signal information, and then uses the PDR to infer the user's trace to monitor the user's motion. Some use PDR technology to trace the user's motion, combined with the WiFi signal distribution information which is gathered in advanced track of the user's indoor location [5]. The Piloc [9] mainly uses PDR to record the user's path and gather the WiFi information along the path, then merge different users' records together to get the WiFi information of the area and then locate and navigate by matching the WiFi information. These methods all work on the base of WiFi information which needs to gather previous, the Piloc makes the gathering easier but can't get rid of it.

The PDR technology mainly uses the accelerometer and magnetic sensor to detect the user's moving direction, use accelerometer to count the user's step number and calculate the moving distance, then use the direction and distance to infer the user's location [10] and [11]. In [10], the author used the acceleration values' changing frequency and amplitude to detect user's step, calculate a step length though the frequency with the help of GPS (when at outdoor), then get the moving distance, and location by matching the indoor map. And in [11], the author used machine learning to detect the user's motion state, improve the accuracy of the detection and can distinguish more kinds of motion, but still needs an indoor map during location. As the PDR method usually has large cumulative error [1], the magnetic field is widely distributed, and there are researches that compared the distribution of WiFi signal and magnetic field, found that the magnetic information can be used as reference for

location and navigation[12], [13] and [14].

III. PROBLEM ANALYSIS

As we need to record the user's walk path and use the path to get back, there are mainly two problems: how to reduce the cumulative error? And how to choose the right turning if there are several turnings of the same direction nearby?

A. Reduce The Cumulative Error

Reduce the accumulation of the error can reduce the total error of the PDR technology. Usually, there are many turnings at a parking port, with the help of these turnings, we can easily reduce the error cumulating.

We use sections to reduce the accumulation of the error as shown in Fig.1, "A----B----C----D" is the user's walk path, A is the car position, the user is at D and wants to get back to A, turning point B and C depart the path into three sections: AB, BC, CD. If we save every section's path length separately, we can navigate at each section separately and the error of different sections won't accumulate.

For example, when user walks back from D to A, in section CD, he walks a length of section CD and gets to C, then turns to BC, and then walks a length of BC, when gets to the B, the error is the section BC's error, the error between C and D has no effect on the error of BC.

B. Get the Right Turning Direction

As shown in Fig.2, if there is more than one turning in a section, like C and C1 in section CD, the PDR technology maybe can't determine which turning to choose.

In Fig.2 (a), the U1 stands for the error of section CD, if C and C1 are far away. U1 is far less than the length of section CD, accorded from the recorded length of section CD, the user can choose the right turning.

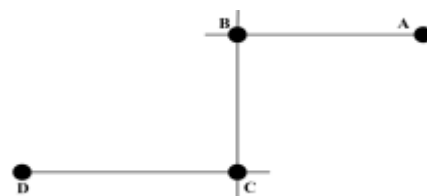


Fig. 1. Reduce the accumulation of error

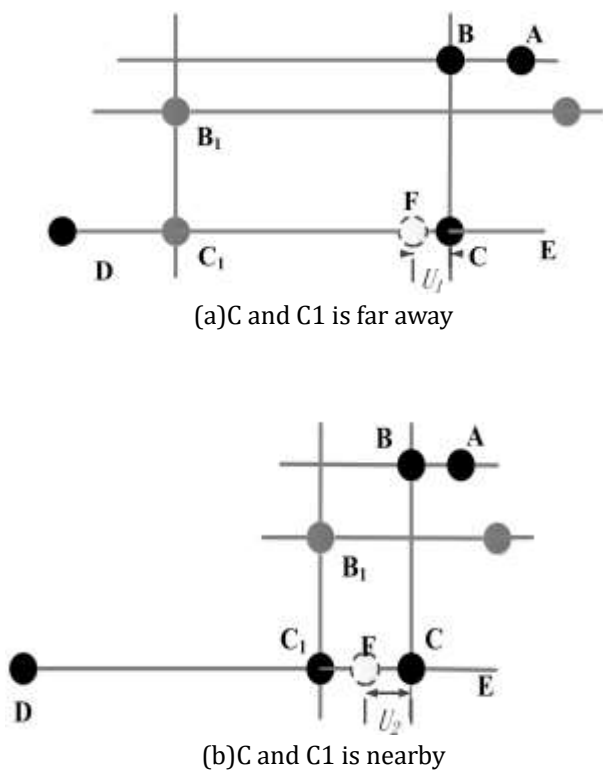


Fig. 2. More than one turning in a section

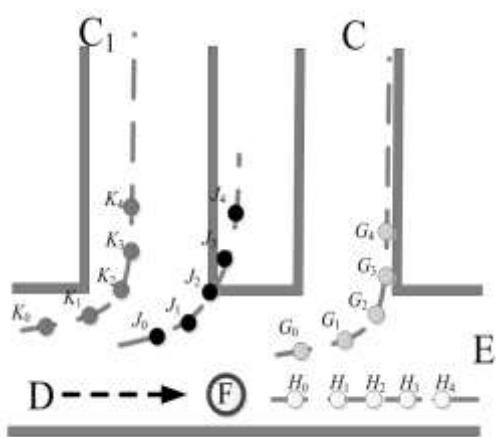


Fig. 3. Magnetic information matching

In Fig.2 (b), the U_2 stands for the error of section CD, if C and C_1 are nearby, U_2 is almost equal to the distance between C and C_1 . For the effect of U_2 , user can't make sure which one is the right turning. Then we need to match the magnetic information of different turnings to get the right turning.

Fig. 3 shows the matching of the magnetic information, when the user passes the turning C first time, the system gets and saves the magnetic information of the turning, use $J_0 \sim J_4$ stands for it. And when the user walks back to C

from D, for the sake of error of CD's length, the user arrives at F, needs to decide which turning to choose. Now the user can collect the magnetic information from D to C_1 which is saved as $K_0 \sim K_4$, and $G_0 \sim G_4$ for D to C, $H_0 \sim H_4$ for D to E. Calculate the similarity between $J_0 \sim J_4$ and $K_0 \sim K_4$, $J_0 \sim J_4$ and $G_0 \sim G_4$, $J_0 \sim J_4$ and $H_0 \sim H_4$ respectively. The most similar one is the right turning.

IV. THE MATCHING ALGORITHM

A. Magnetic Information Gathering and Managing

To record the magnetic information of a turning, we choose five points around a turning, two before the turning and two later and one step one point as shown in Fig.4. The magnetic information got from the magnetic sensor is based on the phone's coordinate system, so we must transform it into the global coordinate system. In this paper we make the North as the direction of y axis, the East as the x axis, and vertical to the horizontal up as the z axis. As shown in Fig 8, let the x_m, y_m, z_m be the data of the phone coordinate, and x_n, y_n, z_n are of the global coordinate, then we get:

$$x_n = x_m \cdot \cos \alpha + y_m \cdot \sin \alpha \tag{1}$$

$$y_n = x_m \cdot \sin \alpha + y_m \cdot \cos \alpha \tag{2}$$

$$z_n = z_m \tag{3}$$

Using the formula (1) (2) (3), we transform the magnetic data into the global coordinate system.

As we have to match the magnetic information we must calculate the similarity of the information. The information of every point is a three vectors value, we can treat it as a point in the global space. Then it changes to calculate the distance of a set of points in the global space. We referred to the DTW algorithm [15] in the template matching problem and adapted it into our system, and designed the following matching rules:

Make $T_0 \sim T_4$ is the set of magnetic information waiting for matching and $J_0 \sim J_4$ is the template. The distance uses the Euclidean distance.

- The matching must be in the order of T_0, T_1, T_2, T_3 and T_4 .
- The matching can't cross. For example, if the T_0 has matched to J_2 , then T_1 can only start matching from J_2 , can't match to J_0 or J_1 .
- The whole distance of the two sets of information is sum of every distance between the matching point and its target point.

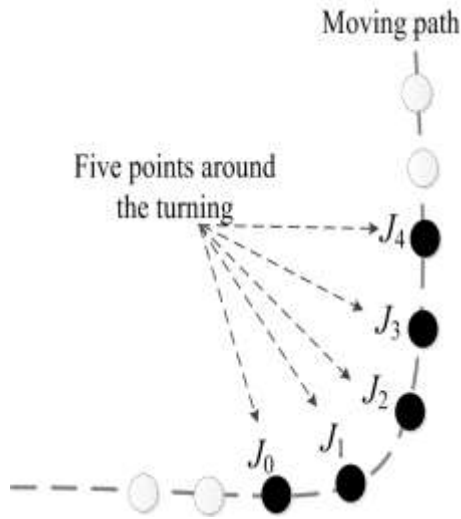


Fig. 1. Gather the magnetic information

In the case of the track based on concrete roadbed, the elastic function is the important factor including the structural performance of track, the durability life, noise,

vibration, etc. Moreover, in the service function, the

uniform strength of roadbed, which is possible and continuity of track rigidity had to be maintained. Therefore, in order to have similar elastic modulus on both sides of the connection section at bridge-earthwork transition zone, it needs to be considered in design [5] and [6].

To evaluate stability of test-bed which was applied with technology of 400km/h class high-railroad infrastructure, connection with PSC Box Bridge and soft ground were selected. The rail fastening device which was used for tracking concrete roadbed in the test-bed was Vossloh System 300-1 and 300W. The settlement and track support rigidity were calculated based on properties 300-1 and 300W.

The value of properties of each rail fastening devices was shown in the table 1. Static rigidity value of the rail fastening system was used to test value in the test certification of SNCF (Societe Nationale des Chemins de fer Francais). The bridge-earthwork connection at transition zone was possible to change deformation of section and

TABLE 1
INPUT DATA FOR RIGIDITY

Category		Input data
Rail	Type	UIC 60 (60EI)
	Mass	78.5 kg/m
	Elastic modulus	2.1×10
	Moment of inertia	$30.55 \times 10^6 mm^4$
Support Rigidity (static/dynamic)	Vossloh System 300-1 (Transition zone 1 and 2)	37/44 kN/mm 33/40 kN/mm
	Vossloh System 300w (Earthwork)	31/40 kN/mm
	Design Axial Load (P)	14tf (HEMU 430x)
	Design Dynamic Wheel Load (Q)	28tf (HEMU 430x)

had the complicated behavior which was moved from the contact point between rail and wheel, so impact coefficient of 2 was used for designing load of dynamic wheel load. The UIC 60 used in EU was shown in figure 1 [7] and [8].

B. Support Rigidity Formula

The formula using track support rigidity at bridge-earthwork transition zone was shown through equations

(1) and (2). These equations were based on continuous longitudinal direction. This support is consisted of ballast, welded rail over support of longitudinal truss rigidity in roadbed and sleeper [9].

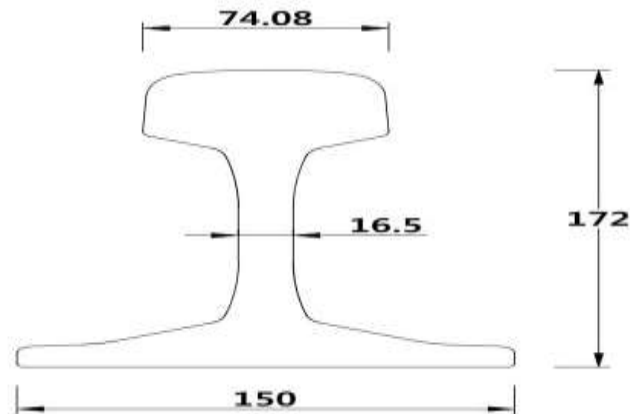


Fig. 1. Section specification of UIC 60

$$K_{stat/dyn} = \sqrt[4]{\left(\frac{4C_c}{a}\right)^3 EI} \quad (1)$$

Then, K (Track rigidity)

C_c (Support point rigidity)
 a (Spacing of sleeper)

$$y_0 = Q/K \quad (2)$$

Then, Q (Wheel force, P/2)

IV. RESULT OF CALCULATION

The vertical displacements (settlement) according to the

rigidity of connection section and earthwork part were shown in the table 2 and figure 2.

The spacing of sleeper and total static rigidity in direction transition zone (PSC Box Bridge) to earthwork were decreased from 650mm to 600mm and from 93.3kN/mm to 86.7kN/mm respectively. The total vertical displacement increased about 0.11mm from 1.47mm to 1.58mm. These results can be forecasted to satisfy recommendation design criterion of 0.3 and do not need to be considered for the additional evaluation for design in bridge-earthwork transition zone [10] and [11].

TABLE 2
 RESULT OF CALCULATION

Category	Unit	Transition Zone 1	Transition Zone 2	Earthwork
Fastening Device	-	Vossloh System 300-1		Vossloh System 300W
Length	M	10	10	
Total Track Support	kN/mm	93.3	90.9	86.7
Spacing of Sleeper	Mm	650	600	600
Static Rigidity	kN/mm	37	33	31
Vertical displacement (Settlement)	mm	1.47	1.51	1.58

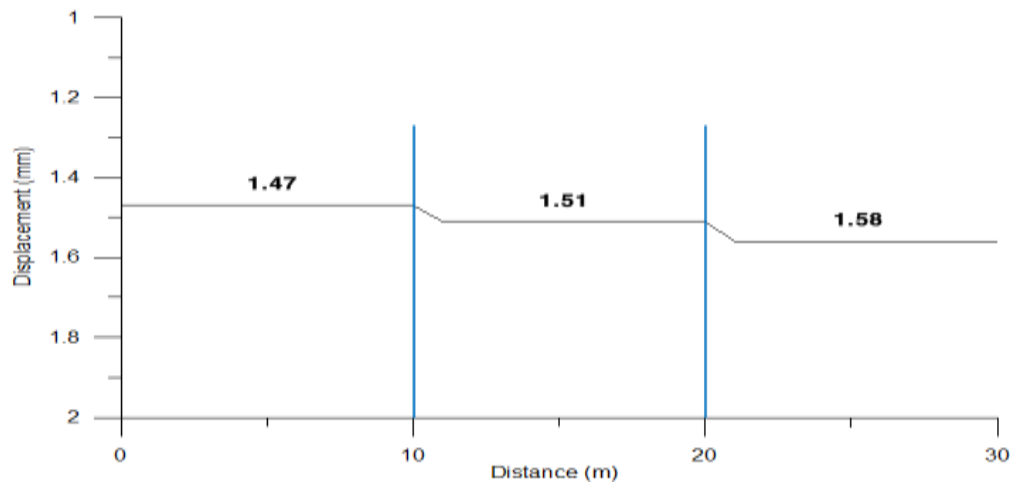


Fig. 2. Vertical displacement (Settlement) by formula

V. MONITORING

The concrete roadbed slab which is the part of bridge and earthwork at transition zone was decided for research site to evaluate the stability on service state of maximum speed and variable operating speed in high-speed train. And monitoring data from transition zone were collected. The research site is the soft ground, which is dramatically changed with the support rigidity coefficient from the top TCL slab to the sub soft ground. It also had the problem of large amount of wheel force variable, which caused critical issue under construction.

C. Specification Of Monitoring Instrument

Two of twelve types of monitoring instruments (sensors) were used to measure structure’s behavior. The name and specifications of the monitoring instrument (Data logger, strain gauge and displacement meter) were shown in the table 3 – 5. When measuring, firstly data recorded in the storage (Throw on data logger) showed No Filtering. And in case the noise was high, the Low Pass Filter more than 1,000Hz was used.

TABLE 3
MONITORING INSTRUMENT

Dynamic Data Logger (CR9000X)	Static Data Logger (CR1000)	Strain Meter (KM-100B)	Displacement Meter(500HCA)
			

TABLE 4
SPECIFICATION OF DATA LOGGER

Category	Specification
Model	CR9000X CR 1000
Resolution	Within 0.0005 Over 0.1
Storage	2Gbyte 128Kbyte
Manufacturer	Campbell

TABLE 5
SPECIFICATION OF MEASURING INSTRUMENT

Category		Specification	
Model		KM-100B	500 HCA
Specification	Resolution	$\pm 5,000 \mu\epsilon$	$\pm 12.70 \text{ mm}$
	Precision	1% RO	0.2% RO
Manufacturer		TML	Schaevitz

D. Location of Installation

The strain gauge was installed in 8 directions of 45° in the neutral axis of the rail web. And it was also located beside 100mm of between the centers of sleeper. Installation location was shown in figure 3.

TCL (track concrete layer) is the concrete roadbed replacing ballast roadbed and HSB (hydraulically stabilized) is the base that is the reinforcing layer of bottom surface.

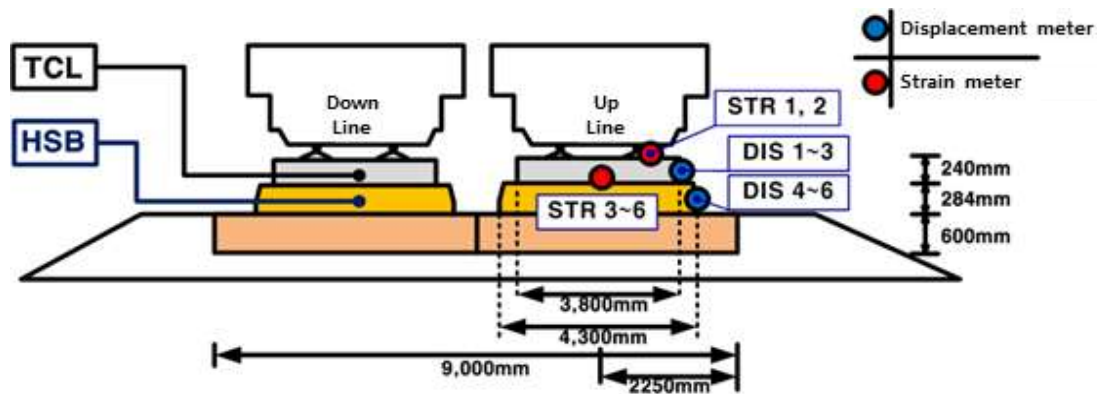


Fig. 3. Front of measuring equipment installation position

Four strain gauges (STR3-6) were installed in the bottom of TCL slab with spacing 2.85m based on the concrete roadbed slab at bridge-earthwork transition zone. This was shown in the figure 4. These locations were based on the upper part of the approach slab where the

transition of rigidity happened with a driving of high-speed train in order to figure out the stability and variation of railroad structure. Additionally, it was installed to calculate flexural tensile stress due to deflection from strain of measuring data.

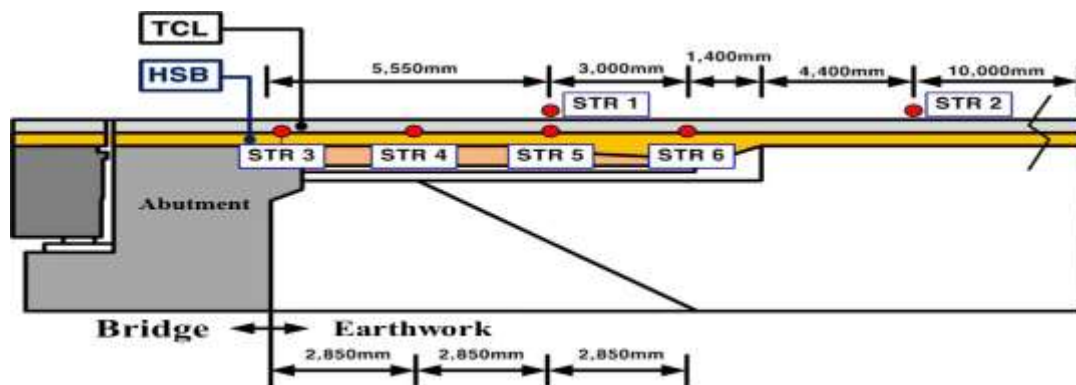


Fig. 4. Side of measuring equipment installation position-strain

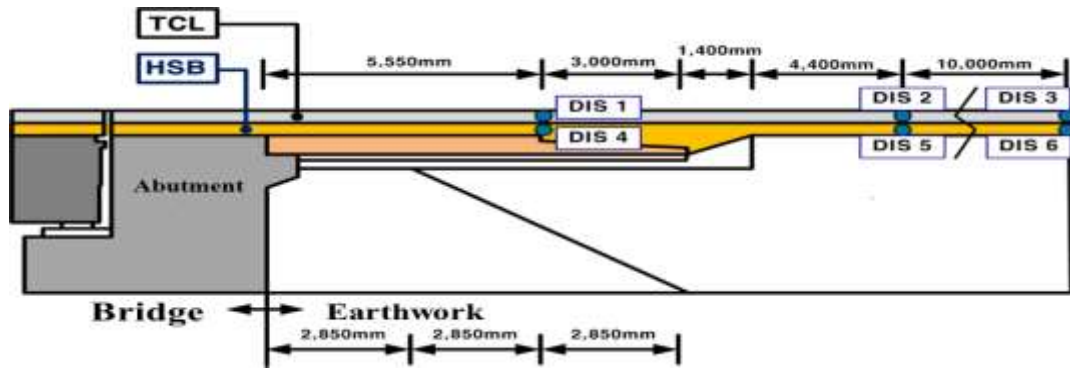


Fig. 5. Side of measuring equipment installation position-displacement meter

The displacement meters were installed three on the center of top approach slab, top of concrete reinforced approach block-earthwork and top of normal earthwork. These locations were shown in the figure 5. When measuring, the train passed through the concrete roadbed slab at bridge-earthwork transition zone with high-speed about over 400km/h. So the proper sampling rate was set for the less of data loss. In order to minimize the noise and error of the data and raise the reliability, low pass filter and high pass filter were set.

E. Measuring Process

The monitoring procedure was performed in the order shown in figure 6. Firstly, the procedure was divided into the previous action step and monitoring step. The former included visual inspection, weather recording of a site and checking malfunction of the sensor and data acquisition. The latter monitoring step was divided into the monitoring according to the train movement and daily monitoring.

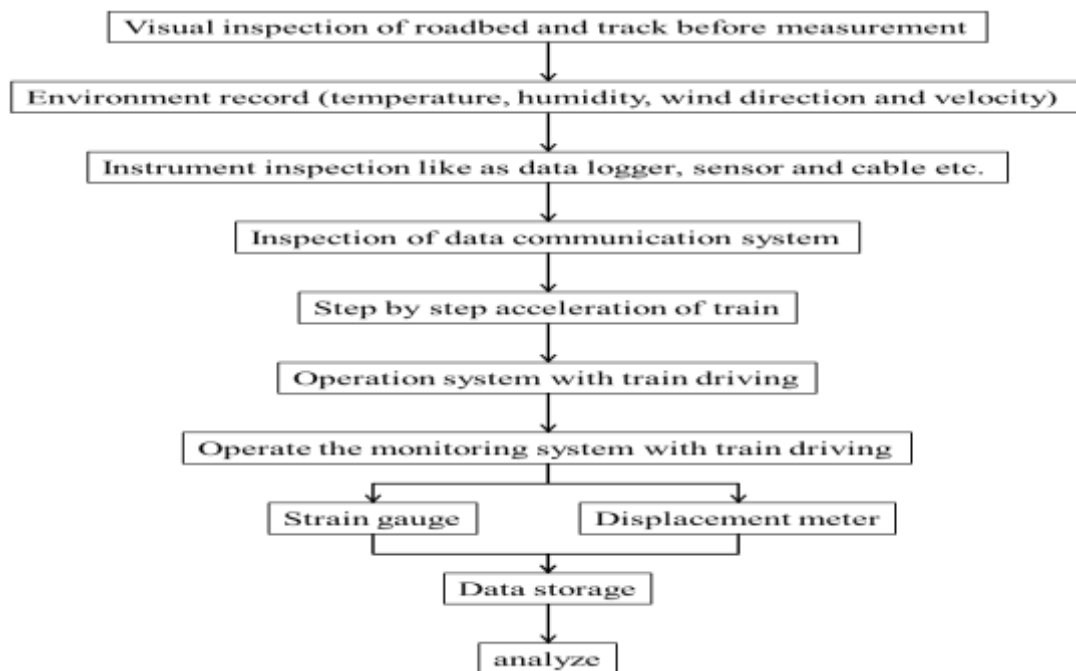


Fig. 6. Monitoring process

F. Criteria of Measurement

For the concrete roadbed slab at bridge-earthwork transition zone, target of monitoring should be

accomplished limit value of displacement and settlement strictly. Especially, the displacement and settlement were important factors for derailment of train. So evaluation of settlement was important also. The criteria of settlement

of slab, rail wheel force and strain of slab were shown in the table 6. Criterion of strain was presented comparing with criteria of shinkansen in Japan. The strain rate gauge is adhered to TCL slab lower part which was between HSB

slab and TCL slab in order to measure bending stress. The criterion of measurement was followed by the driving criterion of Japan, Germany and Korea standard [12] and [13].

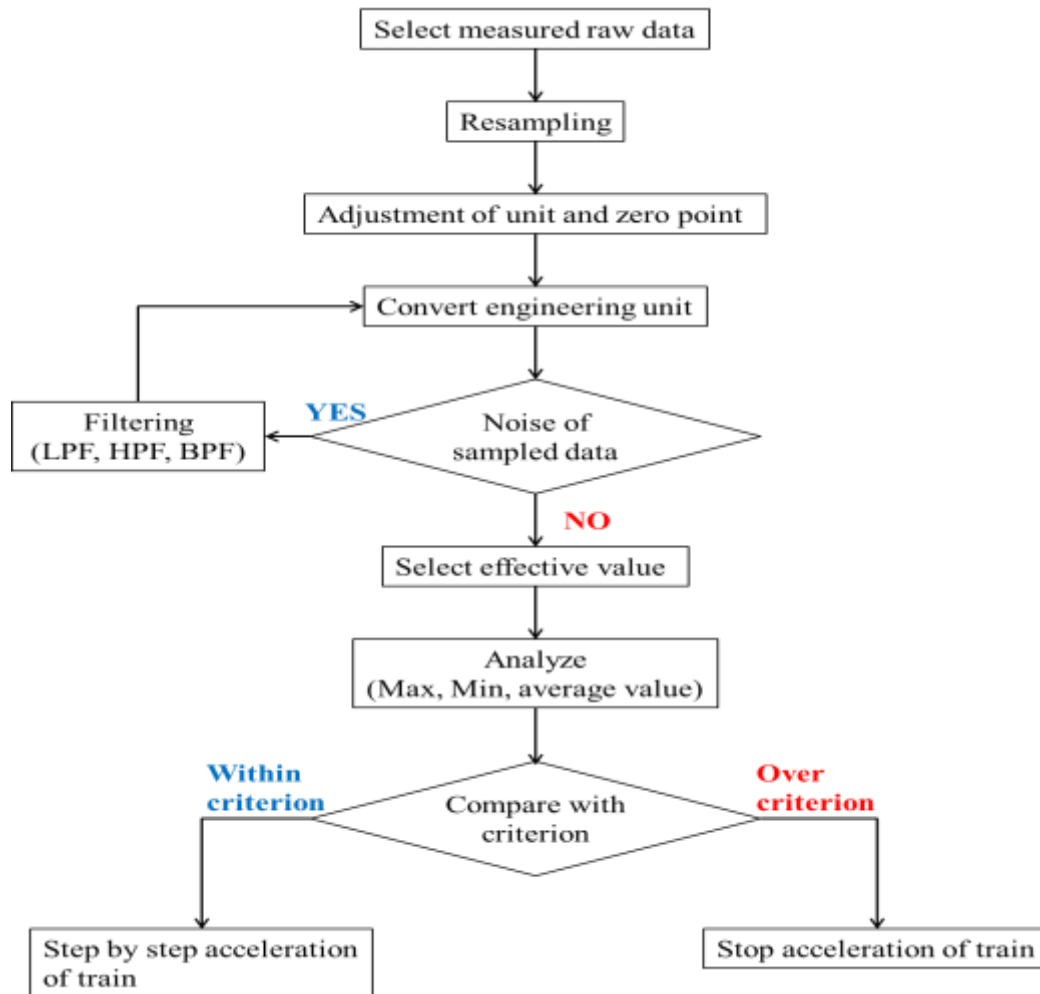


Fig. 7. Algorithm of data conditioning & processing

TABLE 6
CRITERIA OF MEASUREMENT

Subject	Objective	Measurement type	Criterion
Track Support Stiffness	Top slab	Settlement	$\leq 3\text{mm}$
	Rail	Wheel force	$\leq 200\text{kN}$
	TCL Slab	Strain	$\leq 100\mu\epsilon$

IV. RESULT & DISCUSSION

G. Wheel load

Wheel load was reaction of track, fixed infrastructure, with the active forces on the vertical direction by passing

train. And this force can be measured as value and variable of reaction by monitoring. The variable of wheel force by speed change of train in concrete roadbed slab at bridge-earthwork transition zone was shown in the figure 8. Original monitoring plan was measured at maximum

speed, 430km/h, but the speed of train was 400km/h because the train was made for test.

The pattern of wheel load which was increased gradually to 230km/h with acceleration and after approaching peak point, wheel load was decreased gradually according to the acceleration shown. The cause of decreasing wheel load was decreasing its impact coefficient nevertheless of acceleration of train. This phenomenon may have occurred by the vibration of the vehicle (train), central movement of train, deformation of track and train body and wind pressure according to the acceleration of train.

The article [14] about the reduction of wheel load on running speed was performed to measure the component force by speed acting on the rail with installation of the strain gauge on the rail. Then decreasing value with acceleration was induced by analyzing the output according to the combination forces at various locations with normal direction of the track. Same process was applied to the test-bed, and then 3.9kg were decreased according to the increasing 1km/h of speed. This value, 3.9kg per 1km/h, which was major factor for derailment of train, was enough to small value (0.12, variation of wheel load) than value (0.8, variation of wheel load) of stability criteria. So stability of the test-bed was enough too.

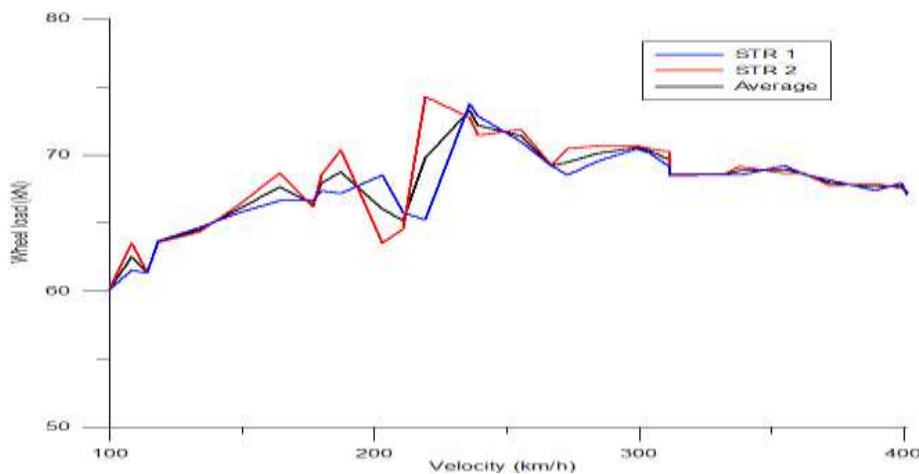


Fig. 8. Wheel Load of driving speed train

In case of calculating the minimum wheel load by using the measured value of STR1 that was 60.134kN, driving speed of 100km/h was considered. The maximum wheel load was 73.744kN at 236km/h, but actual wheel load was 68.60kN at test driving. In the other case of STR2, minimum wheel load was 60.144kN on driving speed of 100km/h. The maximum wheel load was 74.265kN at

236km/h. These values were shown in the table 7. Each maximum value of calculated wheel load was about 34% of 200kN which is design standard of maximum wheel load for high-speed railroad structures. Therefore the stability of railroad structure of test-bed for high-speed railroad was enough to perform its design purpose.

TABLE 7
VALUE OF WHEEL LOAD

Strain Gauge	Max Wheel Load (kN)	Min Wheel Load (kN)	Average Wheel Load (kN)
STR1	73.74	60.14	67.50
STR2	74.26	60.14	67.97
Average	73.25	60.14	67.74

H. Strain of TCL Slab

The TCL slab strain of driving speed was shown in the

figure 9. As to the driving speed of train, the trend was shown to be increasing from 100km/h to 236km/h and decreasing gradually after peak point, 236km/h. The

maximum value was 17.94 $\mu\epsilon$ about 18% of 100 $\mu\epsilon$ which is design standard of maximum strain for high-speed railroad structures. Therefore the stability of

railroad structure of test-bed for high-speed railroad was enough to perform its design purpose.

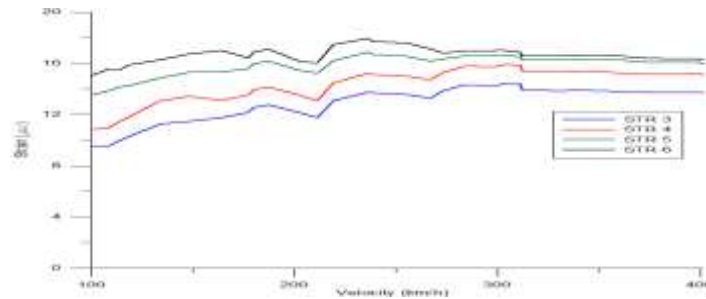


Fig. 9. TCL Slab Strain of Driving Speed Train

The TCL slab stress of driving speed was shown in the figure 10. The bending tensile stress of the slab was calculated using strain data and specification of slab. And the maximum stress was 0.54MPa. In the concrete structure design standard of Korea, in case of being the roadbed compressive strength 50MPa, allowable bending tensile stress should be under 3.7MPa.

The calculated value was about 18% of design standard of maximum strain for high-speed railroad structures. Therefore the stability of railroad structure of test-bed for high-speed railroad was enough to perform its design purpose.

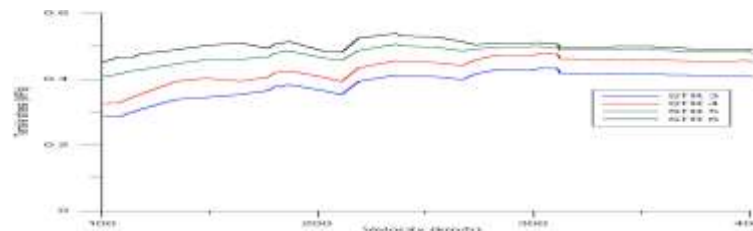


Fig. 10. TCL slab stress of driving speed train

The strain of concrete roadbed at bridge-earthwork transition zone of distance was shown in figure 11. As to strain of distance, it appeared to increase from bridge to earthwork as a bridge. This phenomenon happened to track support rigidity and was decreased from bridge to earthwork so that settlement was increased with strain and stress.

Moreover, it was changed from 13.75 $\mu\epsilon$ to 17.94 $\mu\epsilon$ at 236km/h to 401km/h with low inclination. The wheel load was distributed from concrete abutment of bridge to earthwork, because the approach slab at bridge-earthwork transition zone was connected between bridge and earth. Through this, the structure at transition zone was prevented to face the sudden rigidity transition.

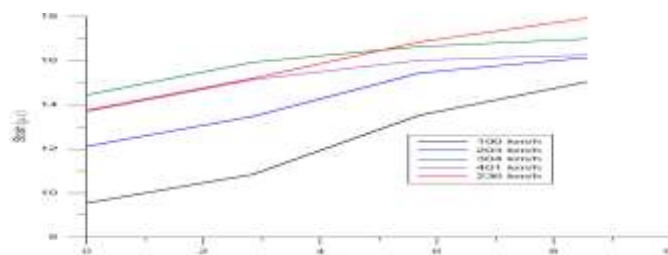


Fig. 11. TCL slab strain of distance

I. Vertical Displacement of Slab

The total vertical displacement of the top slab according to the distance of the bridge-earthwork transition zone was equaled to settlement. The displacement meters were installed three on the center of top approach slab, top of concrete reinforced approach block-earthwork and top of normal earthwork. These locations were shown in the figure 5. The calculated settlement by theory and measured settlement were shown in the figure 12.

Comparing the actually measured value with theoretical, as changing the structure of the support par the similar trend where the displacement increases was shown. In the case of center of top approach slab, the difference of 0.55mm happened. The maximum value of the measured

value was 0.92mm whereas the theoretical result of calculation was 1.47mm. In the case of the top of approach block's upper part, the difference of 0.52mm happened. The maximum value of the measured value was 0.99mm whereas the theoretical result of calculation was 1.51mm. Finally, in normal earthwork, the difference of 0.55mm happened. The maximum value of the measurement was 1.03mm whereas the theoretical result of calculation was 1.58mm. In each part, the theoretical result of calculation and measured value revealed the fixed difference and this difference was the result that it was generated actually in the different wheel load with the calculation. And the vertical displacement was proportionally changed with variation of wheel load.

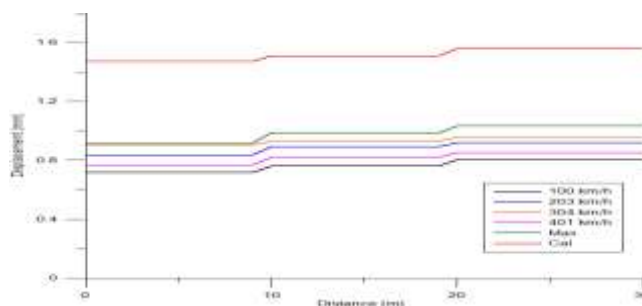


Fig. 12. Vertical displacement of bridge to earthwork

J. Stability Evaluation

The result of stability examination with the measurement assessment was performed comparing the

criteria of measurements. And the concrete roadbed slab at bridge-earthwork transition zone in test-bed satisfied the criteria in environment of driving in 400km/h class of train. The result was shown in table 8.

TABLE 8
RESULT OF STABILITY

Subjective	Objective	Measurement Type	Maximum Value	Criterion	Result
Track	Rail	Wheel load	74.26kN	$\leq 200\text{kN}$	OK
Support	TCL Slab	Strain	17.94 $\mu\epsilon$	$\leq 100 \mu\epsilon$	OK
Rigidity	Top Slab	Settlement	1.03mm	$\leq 3\text{mm}$	OK

V. CONCLUSION

In this research, the stability of the test-bed infrastructure which was applied to the technology of high-speed railroad structure was evaluated according to development of the next generation high-speed train. The test-bed was consisted of connection between PSC Box bridge and earthwork section with concrete roadbed slab at bridge-earthwork transition zone. And by using the

Zimmermann Model, settlement was calculated theoretically. Then, Stability examination with the measurement value was performed.

The theoretical result of total vertical displacement (settlement) according to the track support rigidity of three parts was shown to have a difference of 0.11mm from 1.47mm to 1.58mm. These results can be forecasted to satisfy recommendation design criterion of 0.3 and do

not need to be considered for the additional evaluation for design in bridge-earthwork transition zone.

The results of strain and wheel load test on the concrete roadbed slab at bridge-earthwork transition zone were similar in trend. The wheel load was increased to 236km/h and decreased to 3.9kg per 1km/h with acceleration of train. Additionally, strain was changed from 13.75 $\mu\epsilon$ to 17.94 $\mu\epsilon$ at 236km/h to 401km/h with low inclination by distance of track. These results can be induced; the wheel load was distributed from concrete abutment of bridge to earthwork, because the approach slab at bridge-earthwork transition zone was connected between bridge and earth. Through this, the structure at transition zone was prevented by the sudden rigidity transition.

Maximum ration of Theoretical value of displacement

REFERENCES

- [1] P. Sharp, R. J. Armitage, W. G. Heggie and A. Rogers, "Innovative design of transition zones," in *Proceedings of the International Conference Railway Engineering*, 2002.
- [2] S. Y. Jang and S. C. Yang, "Assessment of train running safety, ride comfort and track serviceability at transition between floating slab track and conventional concrete track," *Journal of the Korean Society for Railway*, vol. 15, no. 1, pp. 48-61, 2012. DOI: [10.7782/jksr.2012.15.1.048](https://doi.org/10.7782/jksr.2012.15.1.048)
- [3] K. Y. Eum, Y. H. Kim and J. W. Kim, "Study on dynamic characteristics of structure approaches by train moving loads," *Journal of the Korean Society for Railway*, vol. 16, no. 4, PP. 298-304, 2013. DOI: [10.7782/JKSR.2013.16.4.298](https://doi.org/10.7782/JKSR.2013.16.4.298)
- [4] S. C. Yang, S. Y. Jang and E. Kim, "Determination of upper limit of rail pad stiffness for ballasted and concrete track of high-speed railway considering running safety," *Journal of the Korean Society for Railway*, vol. 14, no. 6, 526-534, 2011. DOI: [10.7782/JKSR.2011.14.6.526](https://doi.org/10.7782/JKSR.2011.14.6.526)
- [5] VTRC 00-R4, "Guidelines for the use, design, and construction of bridge approach slabs," 1999.
- [6] D. Li and D. Davis, "Transition of railroad bridge approaches," *Journal of Geotechnical and Geoenvironmental Engineering*, vol. 131, no. 11, pp. 1392-1398, 2005. DOI: [10.1061/\(ASCE\)10900241\(2005\)131:11\(1392\)](https://doi.org/10.1061/(ASCE)10900241(2005)131:11(1392))
- [7] UIC Code719R, *Transitions between Structures and Earthworks*, 3rd ed., 2005.
- [8] UIC Code774-3R, *Track & Bridge Interaction* 3rd ed., 2005.
- [9] Ministry of Land and Transport, "Design standards for railway structures and commentary-Limit for displacement," Railway Technology Research Institute, 2006.
- [10] J. Briaud, R. W. James and S. B. Hoffman, "Settlement of bridge approaches (the bump at the end of the bridge)," NCHRP Synthesis 234. Washington D.C, USA, 1997.
- [11] College of Eng, "Movement and settlements of highway bridge approaches," Kentucky Transportation Center, Kentucky, USA, 2002.
- [12] Ministry of Land and Maritime of Korea, "Standards for railway vehicle safety criteria," 2008.
- [13] C. Y. Choi, H. S. Park, K.L. Lee and D.W. Kim, "Management criterion and performance lever of the bridges transitional section in high speed railway," in *Proceeding of the Korea Society for Railway*, 2012, pp. 363-368
- [14] Y.S. Ham. A study on running speed and reduction value in vertical wheel load of rolling stocks," in *Proceeding of the Korean Society of Mechanical Engineers*, 2009, pp. 772-775.

— This article does not have any appendix.—